THE JOURNAL OF BIOLOGICAL CHEMISTRY VOL. 288, NO. 39, pp. 28058–28067, September 27, 2013
© 2013 by The American Society for Biochemistry and Molecular Biology, Inc. Published in the U.S.A.

Exosomes from Retinal Astrocytes Contain Antiangiogenic Components That Inhibit Laser-induced Choroidal Neovascularization*

Received for publication, March 19, 2013, and in revised form, August 6, 2013 Published, JBC Papers in Press, August 7, 2013, DOI 10.1074/jbc.M113.470765

Amir Reza Hajrasouliha[‡1], Guomin Jiang[‡1], Qingxian Lu[‡], Huayi Lu[‡], Henry J. Kaplan[‡], Huang-Ge Zhang[§], and Hui Shao[‡2]

From the [‡]Department of Ophthalmology and Visual Sciences, Kentucky Lions Eye Center and the [§]Department of Research and Development, Robley Rex Medical Center, University of Louisville, Louisville, Kentucky 40202

Background: It is unknown whether the exosomes derived from neurosensory retinal cells regulate angiogenesis in the eye.
Results: Exosomes from retinal astrocytes contain multiple antiangiogenic components that inhibit laser-induced choroidal neovascularization.
Conclusion: Exosomes from monolayer culture of retinal astrocytes, but not retinal pigment epithelium, are antiangiogenic.
Significance: Retinal astrocyte exosomes might be a potential for clinical applications in the treatment of choroidal neovascularization.

Exosomes released from different types of host cells have different biological effects. We report that exosomes released from retinal astroglial cells (RACs) suppress retinal vessel leakage and inhibit choroidal neovascularization (CNV) in a laser-induced CNV model, whereas exosomes released from retinal pigmental epithelium do not. RAC exosomes inhibit the migration of macrophages and the tubule forming of mouse retinal microvascular endothelial cells. Further, we analyzed antiangiogenic components in RAC exosomes using an angiogenesis array kit and detected several endogenous inhibitors of angiogenesis exclusively present in RAC exosomes, such as endostatin. Moreover, blockade of matrix metalloproteinases in the cleavage of collagen XVIII to form endostatin using FN-439 reverses RAC exosome-mediated retinal vessel leakage. This study demonstrates that exosomes released from retinal tissue cells have different angiogenic effects, with exosomes from RACs containing antiangiogenic components that might protect the eye from angiogenesis and maintain its functional integrity. In addition, by identifying additional components and their functions of RAC exosomes, we might improve the antiangiogenic therapy for CNV in age-related macular degeneration and diabetic retinopathy.

Exosomes are nanometer-sized vesicles (30–100 nm in diameter) that are released by cells upon fusion of multivesicular bodies with the plasma membrane (1). Consequently, exosomes contain the proteins, lipids, and RNA, including mRNA and miRNA, of their parent cells. Unlike the fate of proteins trafficked for degradation to the lysosomal system, secreted exosomes are biologically active entities, and their biological information can be delivered into the cells which uptake the exosomes. The effect of exosomes from different cell types varies because the composition of their functional molecules varies depending on their cell of origin. For example, exosomes derived from murine bone marrow-derived dendritic cells are loaded with tumor peptides and display antitumor activity *in vivo* by priming T cells in an antigen-specific manner and stimulating the antitumor activity of cytotoxic lymphocytes (2). By contrast, exosomes secreted by macrophages promote breast cancer invasion and metastasis (3). Exosomes also have the ability to either increase or decrease angiogenesis depending on their origin (4); tumor-derived exosomes play an important role in facilitating metastases by enhancing angiogenesis (5, 6); activated T lymphocyte exosomes also promote angiogenesis, but those from apoptotic T cells inhibit angiogenesis (7). Therefore, different types of exosomes can be used or combined with specific drugs for the therapeutic goal.

Human retina is a delicate organization of neurons, glia (Müller cells, astrocytes, and microglia), and nourishing blood vessels. Retinal vasculature is characterized by an arcuate pattern, sparing the macula of large vessels and absence of retinal vessels from the "fovea" allowing for high visual acuity. Age-related macular degeneration (AMD)[3] is characterized by the abnormal growth of new blood vessels within or beneath the macula and is a leading cause of irreversible blindness among people aged 50 years or older in the developed world. Vascular endothelial growth factor (VEGF) plays an important role in the development of new vessels that originate from the choroid and/or deep capillary bed of the retina and anti-VEGF treatment (such as ranibizumab, bevacizumab, and aflibercept) has

* This work was supported in part by a Research to Prevent Blindness Lew R. Wasserman merit award (to H. S.), an unrestricted grant from Research to Prevent Blindness (to H. J. K.), New York, and the Commonwealth of Kentucky Research Challenge Trust Fund (to H. J. K.).
[1] Both authors contributed equally to this work.
[2] To whom correspondence should be addressed: Kentucky Lions Eye Center, Dept. of Ophthalmology and Vision Sciences, University of Louisville, 301 E. Muhammad Ali Blvd., Louisville, KY 40202. Tel.: 502-852-1329; Fax: 502-852-3183; E-mail: h0shao01@louisville.edu.

[3] The abbreviations used are: AMD, age-related macular degeneration; ANOVA, analysis of variance; CNV, choroidal neovascularization; d*n*, day number; mRMVEC, mouse retinal microvascular endothelial cell; PEDF, pigment endothelium-derived factor; RAC, retinal astroglial cell; RPE, retinal pigment epithelium.

been a major advance in the treatment of this complication of AMD (8, 9). However, >65% of patients do not respond to treatment with improved vision (10), and regrowth of new vessels suggests that pathogenic factors other than VEGF may be involved in the pathogenesis of this complication. These additional factors such as complement (11, 12), cytokines (13, 14), chemokines (10, 15), Toll-like receptors (16, 17), and lipid peroxidation products (18–20) contribute either alone or synergistically to the aberrant angiogenesis. Therefore, an alternative approach that can simultaneously antagonize multiple factors involved in AMD pathogenesis should be explored and may increase the effectiveness of the treatment.

In this report, we tested the hypothesis that cells within the neurosensory retina may release exosomes that regulate angiogenesis. Our results showed that exosomes derived from retinal astrocytes (RACs) of normal mice contain multiple anti-angiogenic factors that inhibit the development of choroidal neovascularization (CNV) in a laser-induced model whereas those derived from retinal pigment epithelium (RPE) do not.

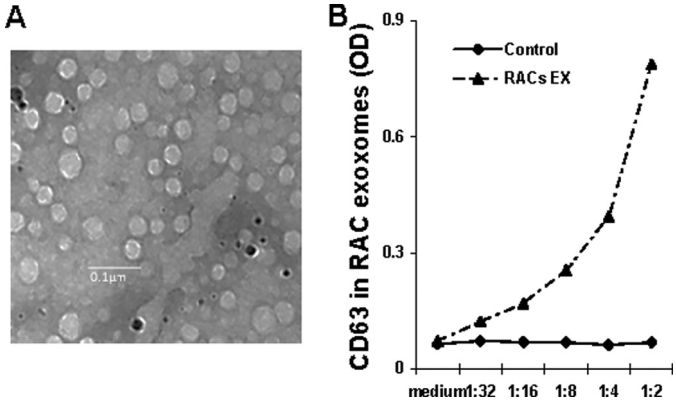

FIGURE 1. **Characterization of RAC-derived exosomes.** *A*, representative electron micrograph of exosomes (magnification, ×72,000; *Scale bar*, 100 nm). Images were acquired with a Phillips CM10 electron microscope. *B*, dose-dependent analysis of exosomes positive for CD63 by ELISA. Purified RAC exosomes (*EX*) were examined in indicated dilutions from the original concentration of 1 μg/ml. The control is the exosome-free cell culture medium.

EXPERIMENTAL PROCEDURES

Animals—Pathogen-free female C57BL/6 (B6) mice, purchased from Jackson Laboratory, were housed and maintained in the animal facilities of the University of Louisville. All animal studies conformed to the Association for Research in Vision and Ophthalmology statement on the use of animals in Ophthalmic and Vision Research. Institutional approval was obtained and institutional guidelines regarding animal experimentation followed.

Mouse Retinal Microvascular Endothelial Cells (mRMVECs)—B6 mRMVECs were purchased from CellBiologics (Chicago, IL) and cultured in mouse endothelial cell culture medium provided by the same company (M1168). 3–5 passage mRMVECs were used.

The isolation and characterization of RACs and RPE cells from B6 mice have been described previously (21, 22). Both cell types were cultured in T75 flask (laminin-coated for RPE) with DMEM (Invitrogen) containing 1 g/liter glucose and supplemented with 10 mM HEPES (pH 7.4), 100 units/ml penicillin, 100 μg/ml streptomycin, and 10% fetal bovine serum (FBS). 3–5 passage RPE and RACs were used for collection of exosomes.

Bone marrow-derived dendritic cells were generated according to a procedure described previously (23). Briefly, bone marrow cells were flushed from femurs of B6 mice and placed at 1×10^6/well in 1 ml of complete RPMI 1640 medium containing 10% FBS and 10 ng/ml granulocyte macrophage-colony-stimulating factors in 24-well plates and fed every other day. On day 6, nonadherent cells were collected for phenotyping. The resulting population consisted of 90–95% dendritic cells as determined by flow cytometry analysis of CD11c. Mouse embryo fibroblasts were provided by Y. Liu (University of Louisville) (24). For exosome collection, all of the cells were grown in a new flask in medium containing exosome-free FBS (see below).

Isolation and Characterization of Exosomes—Cells described above were grown to confluence in medium containing exosome-free FBS, prepared by sequential centrifugation of the FBS at 4 °C at 500 × *g* for 30 min, 15,000 × *g* for 45 min, and 100,000 × *g* for 2 h; then exosomes were purified from the culture supernatant using the same sequential centrifugation procedure (25). The final pellet was resuspended in PBS and the suspension filtered through a 0.22-μm membrane and centrifuged at 100,000 × *g* for 2 h at 4 °C, then the pellet was resuspended in PBS and the protein content determined using a Bradford assay kit (Sigma). For electron microscopy, pellets collected after centrifuging were fixed with 2% paraformaldehyde and loaded on Formvar-coated grids. The samples were negatively stained with phosphotungstic acid for 1 min and examined with Phillips CM10 electron microscopes at 72,000×. Electron microscopy demonstrated that the vesicles present in our preparations were cup-shaped and measured ~30–70 nm in diameter (Fig. 1*A*). ELISA analysis revealed that they were CD63-positive, a marker for exosomes (Fig. 1*B*).

Mouse Model of CNV and Treatment—B6 mice were anesthetized by intraperitoneal injection of ketamine (120 mg/kg) and xylazine (20 mg/kg) and the pupils dilated with a single drop of 1% tropicamide. Krypton red laser photocoagulation (50-μm spot size, 0.05-s duration, 250 mW) was used to generate four laser spots surrounding the optic nerve in one eye per animal using a hand-held coverslip as a contact lens. A bubble formed at each laser spot, indicating rupture of the Bruch's membrane (26). For treatment, mice were injected periocularly with 10 μl of PBS alone or PBS containing 2 μg of exosomes starting on the day of CNV induction (d1) either daily or every other day until d7 (end of the experiment).

Labeling of Exosomes—RAC-derived exosomes were labeled with the red fluorescent dye PKH26 using a commercially available kit (Sigma-Aldrich) according to the manufacturer's instructions.

CNV Observation by Fluorescence Microscopy and Choroidal Flat Mounts—Seven days after rupture of the Bruch's membrane, the mice were anesthetized and perfused via the tail vein with 50 mg/ml fluorescein isothiocyanate-labeled dextran (FITC-dextran; 2×10^6 average molecular mass; Sigma-Aldrich). After pupil dilation using 0.5% tropicamide and 1.25% phenylephrine hydrochloride ophthalmic solutions, retinal

vascular leakage was examined under a fluorescence microscope (Eclipse E600; Nikon) and photographed. Animals were then sacrificed and the eyes dissected and fixed overnight in 4% paraformaldehyde. Choroidal-retinal flat mounts were prepared and examined under a fluorescence microscope (HAL-100; Zeiss). Axiovision Rel, 4.8 software (Zeiss) was used to measure the total area of CNV at each rupture site by personnel blind to study treatment and control groups.

Identification of F4/80-positive Macrophages in the Laser-treated Spots—Choroidal-retinal flat mounts prepared from FITC-dextran-injected mice were fixed with ethanol, washed with PBS, and blocked by incubation for 1 h at room temperature in PBS containing 3% BSA. They were then incubated overnight at 4 °C with rat monoclonal antibody against mouse F4/80 (1:100; eBiosciences, San Diego, CA) in PBS containing 1% BSA. Negative control sections were treated identically, but the primary antibody was omitted. After rinse, the specimens were incubated for 1 h at room temperature with Cy3-conjugated donkey anti-rat IgG antibodies (Jackson ImmunoResearch Laboratories) in PBS containing 1% BSA. Then the number of positive cells was counted and representative images photographed.

Isolation and Culture of Murine Peritoneal Macrophages—B6 mice were injected intraperitoneally with 5 ml of sterile RPMI 1640 medium, and peritoneal cells were harvested as described previously (27). The cells were suspended in antibiotic-free RPMI 1640 medium containing 10% FBS and incubated in a humidified incubator at 37 °C in 5% CO_2 in 24-well cell culture plates for 2 h, then nonadherent cells were removed and the medium replaced. The resultant cell preparation consisted of >85% macrophages, as verified by flow cytometric analysis of cells immunostained with antibodies against mouse F4/80 and MHC class II molecules (BioLegend, San Diego, CA).

Chemotaxis Assay—Peritoneal macrophages (3×10^5 cells/well) were added to the upper well of a microchemotaxis device (5-μm pore size; 24-well; Transwell; Corning-Costar), and RPMI 1640 medium containing chemokine (C-C motif) ligand 2 (CCL-2; 10 nM, BioLegend) was added to the lower well with or without exosomes, and the cells that migrated to the lower well after 2 h were collected and counted by flow cytometry (28). All assays were performed in triplicate.

Migration Assay of mRMVECs—mRMVECs were cultured to 95% confluence in the 6-well plates. A crossed lesion was made using a cell scraper. Cells were rinsed three times with serum-free medium and incubated with the medium with increasing doses of RAC-derived exosomes. After 24 h of migration, three randomly selected fields at the lesion border were acquired using a 10×phase objective on an inverted microscope (Olympus IMT2; Tokyo, Japan). Using image, the distance between the margin of the lesion and the most distant point on migrating cells was analyzed.

VEGF-induced mRMVEC Proliferation by BrdU Staining—mRMVECs (1×10^4/well) were cultured with VEGF (50 μg/ml) in 500-μl total volume in the presence of increasing doses of RAC exosomes in 6-well plate chamber slides. After 24 h, BrdU (20 μM) was added to each well and cultured for additional 12 h. The proliferative cells were detected using FITC-labeling BrdU antibody and counted at five randomly selected fields in each well under a 5× lens.

VEGF-induced mRMVEC Tubule Forming Assay—mRMVECs were seeded (5000 cells/well) in a Matrigel-coated 96-well plate (BD Biosciences) in the medium or medium containing 50 μg/ml VEGF in the increasing doses of RAC-derived exosomes and incubated up to 8 h at 37 °C. Tube formation was examined every 2 h under an inverted microscope and photographed at 40× magnification. Tubule complexity number and branch length were measured using ImageJ software (National Institutes of Health). Results are the mean ± S.E. of triplicate experiments.

Mouse Angiogenesis Antibody Array Analysis—Exosomes of RACs and RPE were extracted and transferred to radioimmune precipitation assay buffer (Sigma) with protease inhibitor mixture (Sigma). 300 μg of each sample was subjected to Mouse Angiogenesis Protein Array (R&D Systems, ARY015). Data were analyzed using ImageJ software and graphed as bar charts.

Western Blotting—RAC cells were treated with or without 300 μg/ml FN-439 on days 0 and 3 of subculture. Exosomes were then extracted and transferred to radioimmune precipitation assay buffer with protease inhibitor mixture (Sigma), and Western blotting was performed using Endostatin primary antibody (1:500; R&D Systems) and secondary anti rat-HRP (1:10,000; Santa Cruz Biotechnology).

Statistical Analysis—Experiments were repeated at least two times. Statistical comparisons were made using an unpaired Student's t test for two sets of data, a one-way or two-way ANOVA for three or more means, and χ^2 test for analyzing the incidence of retinal vascular leakage. Values determined to be significantly different from those for controls are marked with asterisks in the figures (*, $p < 0.05$; **, $p < 0.01$).

RESULTS

Exosomes Rapidly Reach the Retina after Subtenon Injection—Intravitreal injection of anti-VEGF agents is routinely performed clinically. However, it can be associated with significant complications, such as infectious endophthalmitis. Therefore, we first decided to study the ability of exosomes, which are nanometer-sized particles, to reach the retina following extraocular (*i.e.* subtenon) injection. Mice were injected via the tail vein with FITC-dextran (*green*) to identify blood vessels, then injected periocularly with PKH26-labeled RAC-derived exosomes (containing 10 μg of protein) and kinetically observed *in vivo* with the fluorescent microscope. As documented in Fig. 2, the labeled exosomes (*red*) started to be seen in the neural retina 15 min after injection (Fig. 2*A*), gradually increased at 30 and 60 min (Fig. 2, *B* and C) and then more diffusely throughout the neural retina (Fig. 2*D*). Thus, we observed that the subtenon injection of exosomes resulted in a rapid and diffuse spread of these microparticles within the neurosensory retina. Fig. 2, *E* and *F*, showed that at 60 min after exosome injection, PKH26-labeled exosomes were detected in the retina and the choroid adjacent to the area of extrascleral injection, as well as laser photocoagulation.

RAC-derived Exosomes Inhibit CNV—We then evaluated the effect of RAC-derived exosomes on laser-induced retinal vascular leakage and CNV. RAC-derived exosomes were injected

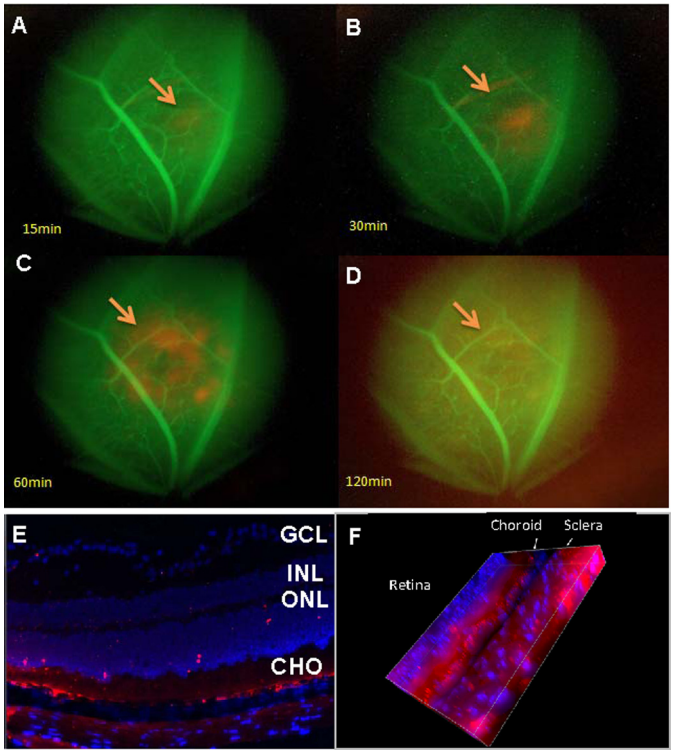

FIGURE 2. **Periocular injected exosomes reach the choroid-retina.** *A–D*, time course of the appearance of exosomes in the eye as seen by fluorescent microscopy. Mice preinjected with FITC-dextran, which labels blood vessels green, were injected periocularly with PKH26-labeled RAC-derived exosomes (10 μg) and examined *in vivo* using fluorescence microscopy at 15 (*A*), 30 (*B*), 60 (*C*), and 120 (*D*) min after injection (magnification, ×10). The *arrows* indicate PKH26-labeled (*red*) exosomes. *E* and *F*, confocal microscope of two-dimensional (*E*) and three-dimensional (*F*) view of frozen sections of the retina and choroid prepared after sacrifice of mice 60 min after periocular injection of RAC-derived exosomes labeled with PKH26 (*red*) (magnification, ×40; the *blue stain* of nucleus is DAPI. *E*, *GCL*, layer of ganglion cells; *INL*, inner nuclear layer; *ONL*, outer nuclear layer; *CHO*, choroid.

in the subtenon space (2 μg of protein/dose) either daily or every other day starting on the day of laser burn (d1). On day 7 FITC-dextran was injected via the tail vein to identify the retinal vascular leakage by *in vivo* fluorescent microscopy. As seen in Fig. 3*A*, control eyes treated with PBS had a 42% incidence of retinal vascular leakage, whereas mice injected daily with RAC-derived exosomes showed no retinal vascular leakage (0/24, 0% incidence), similar to laser-untreated and PBS-injected control retina; treatment every other day was less effective (25% of incidence) than daily treatment. Choroidal flat mounts were then performed to examine CNV formation of RAC exosome treatment. Although every other day was not as effective as daily treatment it did result in a dramatic reduction in the area of choroidal neovascularization (Fig. 3*B*).

To determine whether the late treatment (*i.e.* from day 7 to 14 after laser injury) of RAC-derived exosomes could reduce laser-induced CNV, we used the same mode of injection starting from day 1 to day 7 to inject RAC-derived exosomes from day 7 to 14. As shown in Fig. 3*C*, treatments starting day 7 had treatment efficacy similar to those starting day 1, both early and late treatments of RAC-derived exosomes having significantly fewer areas of CNV than the one with PBS treatment.

RAC-derived Exosomes Are the Most Effective in Inhibiting CNV—To determine whether inhibition of retinal vascular leakage and CNV was specific to RAC-derived exosomes, we compared the efficacy of daily injection of 2 μg of exosome-derived RACs, RPE cells, or two nonretinal tissue cells (fibroblasts and dendritic cells). As shown in Fig.4, among all of the exosomes tested, only RAC-derived exosomes significantly suppressed retinal vascular leakage (Fig. 4, *A* and *B*) and reduced CNV (Fig. 4*C*), whereas those derived from fibroblasts, dendritic cells, or RPE cells did not significantly alter laser-induced retinal vascular leakage and the area of CNV examined by *in vivo* fluorescent microscopy and choroid flat mount, respectively.

RAC-derived Exosomes Reduced the Number of Macrophages in CNV- and CCL-2-induced Macrophage Migration—The major inflammatory cells identified in the CNV complex in AMD are the macrophages (29). We investigated the effect of RAC-derived exosomes on macrophage infiltration into the choroid of the laser-induced CNV complex. Choroidal flat mounts were stained with Cy3-conjugated antibody against F4/80, a macrophage-specific marker. The number of F4/80-positive cells in the choroidal scar was counted following the subtenon injection of 2 μg of RAC-derived exosomes on a daily basis. As shown in Fig. 5*A*, the mean number of macrophages per laser spot on day 7 was 60.8 (±13.6) in the PBS-treated group compared with 27.2 (±4.4) in the RAC-derived exosome-treated group, a significant reduction of 55% ($p < 0.01$).

Further, we performed an *in vitro* chemoattractant migration assay using peritoneal macrophages to confirm that RAC-derived exosomes can inhibit macrophage migration. Peritoneal macrophages were stained with antibodies against MHC class II and F4/80, two markers for macrophages (Fig. 5*B*). Macrophages were added to the top well of a chemotaxis chamber, and the macrophage chemoattractant CCL2 (10 nM), either alone or with RAC-derived exosomes (1 μg/ml or 10 μg/ml), was added to the lower well. The number of cells that migrated to the lower well after 2 h was counted by flow cytometry. As shown in Fig. 5*C*, CCL2-induced macrophage migration was reduced by RAC-derived exosomes in a dose-dependent manner.

RAC-derived Exosomes Inhibit mRMVEC Migration and Vascular Tubule Forming in Vitro—To determine whether RAC-derived exosomes would target vascular endothelial cells, we examined RAC-derived exosomes on migration, proliferation, and tubule forming of mRMVECs. As illustrated in Fig. 6, RAC-derived exosomes at a dose of 1 μg/ml significantly reduced the migration of mRMVECs (Fig. 6*A*), but not EC proliferation (Fig. 6*B*). Moreover, RAC-derived exosomes inhibited VEGF-induced tubule network forming in a dose-dependent manner, with both the number of branch points (Fig. 6*C*) and total branch length being significantly reduced (Fig. 6*D*).

RAC-derived Exosomes Express Elevated Levels of Antiangiogenic Proteins—To identify the molecules in the exosomes derived from RACs that can inhibit retinal vascular leakage and new choroidal vessel formation, we analyzed the expression of 53 pro- or antiangiogenesis proteins in the exosomes from RAC, using exosomes from RPE, which did not have significant inhibitory effects on laser-induced CNV, as a comparison. The

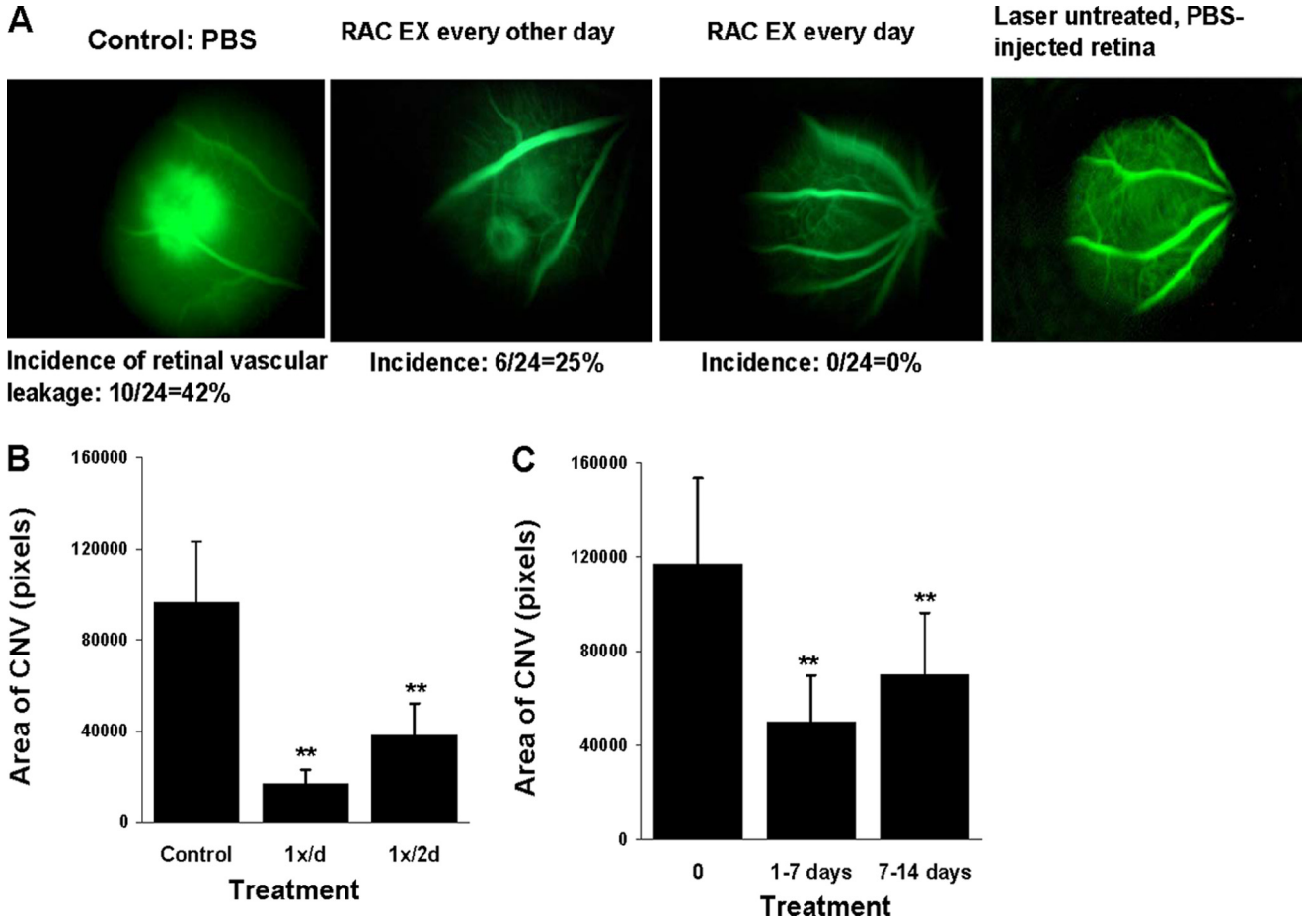

FIGURE 3. **RAC-derived exosomes inhibit retinal vascular leakage and choroid new vessel formation in a laser-induced CNV model.** *A* and *B*, periocular injection of PBS (control) or RAC-derived exosomes (2 μg) was performed every other day or every day ($n = 6$ mice/group) starting at the same day of laser injury (d1). On day 7, retinal vascular leakage was determined *in vivo* by fluorescence microscopy (*A*) and average area of CNV in all four laser spots of six mice measured in choroidal flat mounts (*B*). *C*, on day 14, average area of CNV was determined in the mice treated with PBS or daily with RAC-derived exosomes from day 1 to 7 or from day 7 to14. **, $p < 0.01$ compared with control group treated with PBS in one-way ANOVA. *Error bars*, S.E.

results in Fig. 7 showed the differences of angiogenesis regulator expression between exosomes derived from RACs and RPE. Endostatin, KC (CXCL-1), MIP (macrophage inflammatory protein)-1α, MMP (matrix metalloproteinase)-3 and MMP-9, Nov (nephroblastoma-overexpressed), and PEDF (pigment endothelium-derived factor) were exclusively expressed in RAC-derived exosomes. In addition, proliferin and TIMP-1 (tissue inhibitor of metalloproteinases) were expressed higher in RAC exosomes than in RPE exosomes. In contrast, RPE exosomes exclusively expressed ET-1 (endothelins) and PIGF-2 (placenta growth factor-2) and expressed higher levels of PTX3 (pentraxin-related protein, also known as TNF-inducible gene 14 protein) than RAC exosomes. Among up-regulated expression of proteins in RAC-derived exosomes, endostatin, PEDF, and TIMP-1 are recognized as antiangiogenic factors. PlGF-2 in RPE-derived exosomes is more related to vascular endothelial growth factor (VEGF). The higher concentrations of endostatin and PEDF in RAC exosomes than those in RPE exosomes were further confirmed by ELISA (Fig. 7*C*).

Endostatin Is Responsible for Suppression of Retinal Vascular Leakage—Endostatin is known as an endogenous inhibitor of angiogenesis. To determine whether endostatin is the one in RAC exosomes responsible for inhibition of angiogenesis induced by laser injury in the choroid, we used FN-439, a MMP inhibitor to block MMPs in the cleavage of collagen XVIII to form endostatin (Fig. 8*A*). RACs after treatment with FN-439 released the exosomes which contained the reduced level of endostatin compared with the endostatin in the exosomes from RACs without treatment. RPE exosomes did not express endostatin, consistent with the array result. Further, we injected the exosomes from RACs treated with or without FN-439 into laser-induced CNV mice. Fig. 8, *B* and *C*, showed that retinal vascular leakage was suppressed after treatment with RAC exosomes, and FN-439 completely reversed the effect (33%, 0%, 30%, $p < 0.05$, Fig. 8, *B* and *C*), whereas the inhibition of RAC exosomes on choroidal neovascularization area could not be fully reversed by FN-439-treated exosomes (Fig. 8, *D* and *E*). The results suggested that endostatin alone is responsible for suppression of retinal vascular leakage but not reduction of CNV area.

Internalization of Exosomes by Macrophages and mRMVECs—To determine the mechanisms of RAC exosomes targeting macrophages and vascular endothelial cells, we examined the internalization of exosomes by these two cell types. Macrophages and mRMVECs were co-cultured with PKH67-labeled exosomes from either RACs or RPEs and analyzed by fluores-

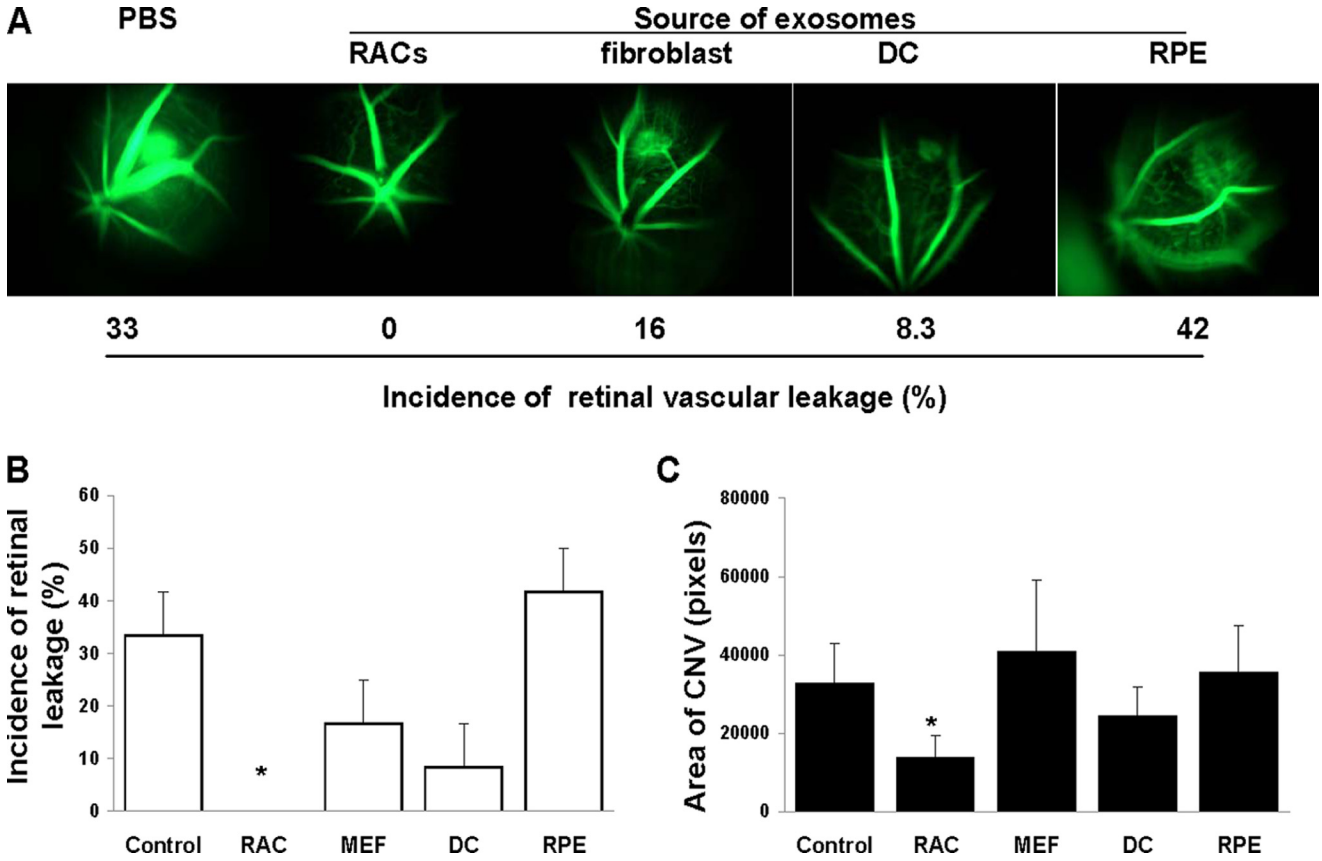

FIGURE 4. **Exosomes derived from RACs are the most effective in suppressing active CNV.** Exosomes (2 μg) derived from RACs, RPE, fibroblasts, dendritic cells (DCs), or PBS (control) were injected periocularly daily into mice with laser-induced CNV, then, after 7 days, retinal vascular leakage was determined *in vivo* by fluorescence microscopy (*A* and *B*) and average area of CNV in all four laser spots of six mice measured in choroidal flat mounts (*C*). *, $p < 0.05$ compared with control group treated with PBS in one-way ANOVA. *Error bars*, S.E.

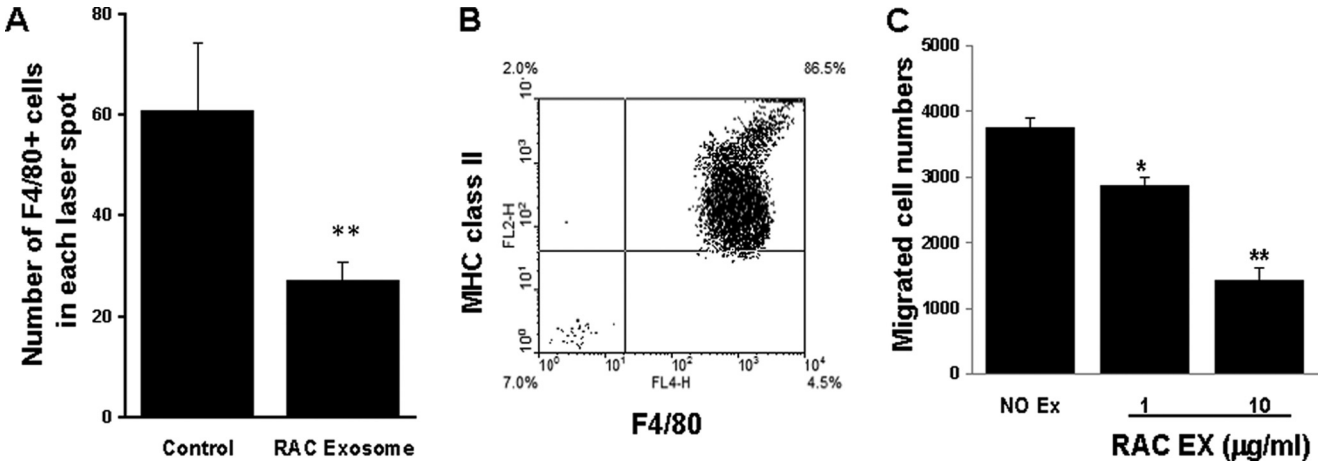

FIGURE 5. **RAC-derived exosomes reduced the number of F4/80$^+$ macrophages in the area of the laser-induced choroidal injury and in an *in vitro* chemoattractant migration assay.** *A*, mice injected daily with 2 μg of RAC-derived exosomes were examined on day 7 for infiltrated macrophages in the choroidal flat mount using Cy3-conjugated F4/80 antibody; the average of infiltrated F4/80-positive macrophages per laser spot was counted and calculated ($n = 24$ laser spots). *B* and *C*, peritoneal macrophages, 86.5% pure (*B*) at the top well of a chemotaxis chamber that migrated to the lower wells containing the macrophage chemoattractant CCL2 (10 nM), alone or together with 1 or 10 μg/ml of RAC-derived exosomes, were collected after 2 h incubation and counted by flow cytometry (*C*). *, $p < 0.05$; **, $p < 0.01$ compared with control group treated with PBS in one-way ANOVA. *Error bars*, S.E.

cent microscopy. After 2 h, exosomes were detected within macrophages and mRMVEC (Fig. 9).

DISCUSSION

Exosomes released by circulating cells (*e.g.* leukocytes and platelets), endothelial cells, and tumor cells have been demonstrated to have effects on angiogenesis, with most studies reporting that exosomes promote angiogenesis both *in vitro* and *in vivo* (4). We have shown, for the first time, that exosomes released from the neurosensory retina, specifically, RACs, can suppress retinal vascular leakage and inhibit choroid neovascularization in a laser-induced mouse model, whereas exosomes

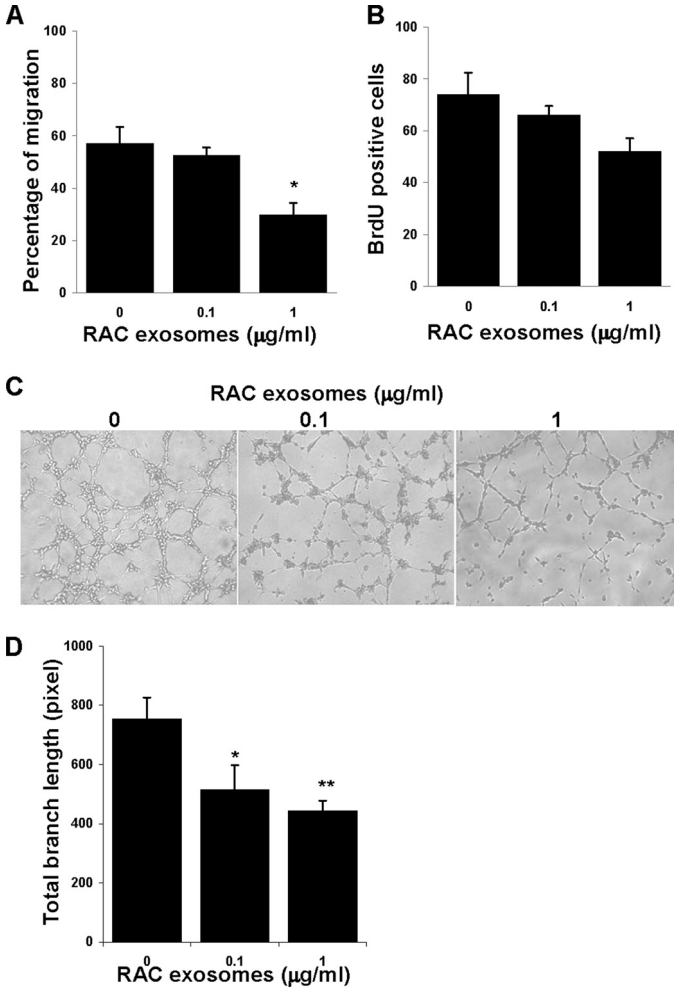

FIGURE 6. **RAC exosomes inhibited the migration and vascular tubule forming, but not proliferation of mRMVECs.** *A*, migration of mRMVECs. A crossed lesion was made in the 6-well plates cultured with 95% confluence mRMVECs in the medium with increasing dose of RAC exosomes. After 24 h of migration, three randomly selected fields at the lesion border were acquired using a 10× phase objective on an inverted microscope, and the distance between the margin of the lesion and the most distant point on migrating cells was analyzed. *B*, proliferation of mRMVECs. mRMVECs were cultured with 50 μg/ml VEGF in the presence of increasing doses of RAC exosomes. After 24 h, 20 μM BrdU was added to each well and cultured for additional 12 h. The green BrdU-positive proliferated cells were counted at five randomly selected fields in each well under a 5× lens. *C* and *D*, tubule forming of mRMVECs. mRMVECs were cultured as in *B* but for 6 h. Representative examples of micrographs (*C*) and total branch length (*D*) are shown. Data are mean ± S.E. (*error bars*) of triplicate experiments. *, $p < 0.05$; **, $p < 0.01$ compared with control group treated without RAC exosomes in one-way ANOVA.

derived from RPE cannot. The results of these studies indicate that in the eye, exosomes derived from different ocular cells may be important for the balance of anti- and proangiogenesis in this area and the integrity of vision function. They may also play a role in the evolution of AMD and the other angiogenetic related conditions. The ability of exosomes from neurosensory retina to influence angiogenesis may be useful as an adjunctive therapy in several diseases including exudative AMD, proliferative diabetic retinopathy, and angiogenesis associated with tumor metastasis. However, although we did not observe antiangiogenic activity from the exosomes derived from the RPE cell monolayer culture in the flask, it is possible that secretion of RPE exosomes from the apical or basal surface may have a different property.

The mechanisms by which RAC exosomes suppress retinal vascular leakage and inhibit choroid neovascularization in a laser-induced mouse model might be that RAC exosomes target both macrophages and vascular endothelial cells. Infiltrating macrophages play an important role in exudative AMD (30, 31) and in experimental CNV (32, 33). They are a major source of inflammatory cytokines, complement, and VEGF, all of which are important in the pathogenesis of inflammation and new vessel formation. RAC-derived exosomes suppressed the infiltration of macrophages into laser treated areas (Fig. *5*) and inhibited the migration of macrophages in a chemotactic chamber. In addition to the direct effect of RAC-derived exosomes in reducing the number of infiltrating macrophages, the components of these exosomes may directly antagonize both the inflammatory and angiogenic factors released from these cells. RAC exosomes also target vascular endothelial cells. Our *in vitro* study showed that RAC exosomes inhibited the migration and vascular tubule forming of mRMVECs, but inhibited proliferation only minimally.

The antiangiogenic effect of RAC exosomes on macrophages and vascular endothelial cells might be contributed by their multiple molecules, including proteins, lipids, mRNA, and miRNA, which are likely operate collaboratively in preventing and inhibiting angiogenesis. Profiling angiogenic related protein expression with antibody array analysis of exosome extracts revealed that endostatin, PEDF, and TIMP-1, chemokines of KC (CXCL-1), and MIP (macrophage inflammatory protein)-1, as well as matrix metalloproteinase, such as MMP-3 and MMP-9, are exclusively or highly expressed on RAC exosomes. Endostatin, PEDF, and TIMP-1 are known to possess antiangiogenic properties (34–37), whereas these chemokines and MMPs can either promote or inhibit angiogenesis, depending on their environmental context. For example, MMPs promote angiogenesis by increasing the bioavailability of the proangiogenic growth factors VEGF, fibroblast growth factor 2 (FGF-2), and TGF-β (38). These factors stimulate proliferation and migration of endothelial cells. On the other hand, MMPs act antiangiogenically through cleavage of plasminogen and collagen XVIII, resulting in generation of the antiangiogenic factors angiostatin and endostatin (38). Mice lacking collagen XVIII/endostatin have large CNV lesions and increased vascular leakage compared with control wild-type mice after laser burn induction (34). We further validated endostatin and PEDF expression in RAC exosomes by ELISA and its antiangiogenic function by using endostatin-free RAC exosomes in laser-induced CNV. Because there is no neutralizing endostatin antibody commercially available, we used MMP inhibitor, FN-439, to block MMP for cleavage of collagen XVIII to generate endostatin. Our data demonstrated FN-439 reduced endostatin in RAC exosomes, and these exosomes, like endostatin-free RPE exosomes, could not suppress vascular leakage, indicating that endostatin in RAC exosomes is responsible for preventing vessel leakage; however, endostatin alone could not suppress the formation of CNV (Fig. 8). This finding suggests that endostatin is more sensitive in inhibiting vascular leakage than the size of CNV and that multiple factors such as PEDF in RAC exosomes are involved in the inhibition of CNV formation. The mechanism that through which endostatin inhibits retinal vas-

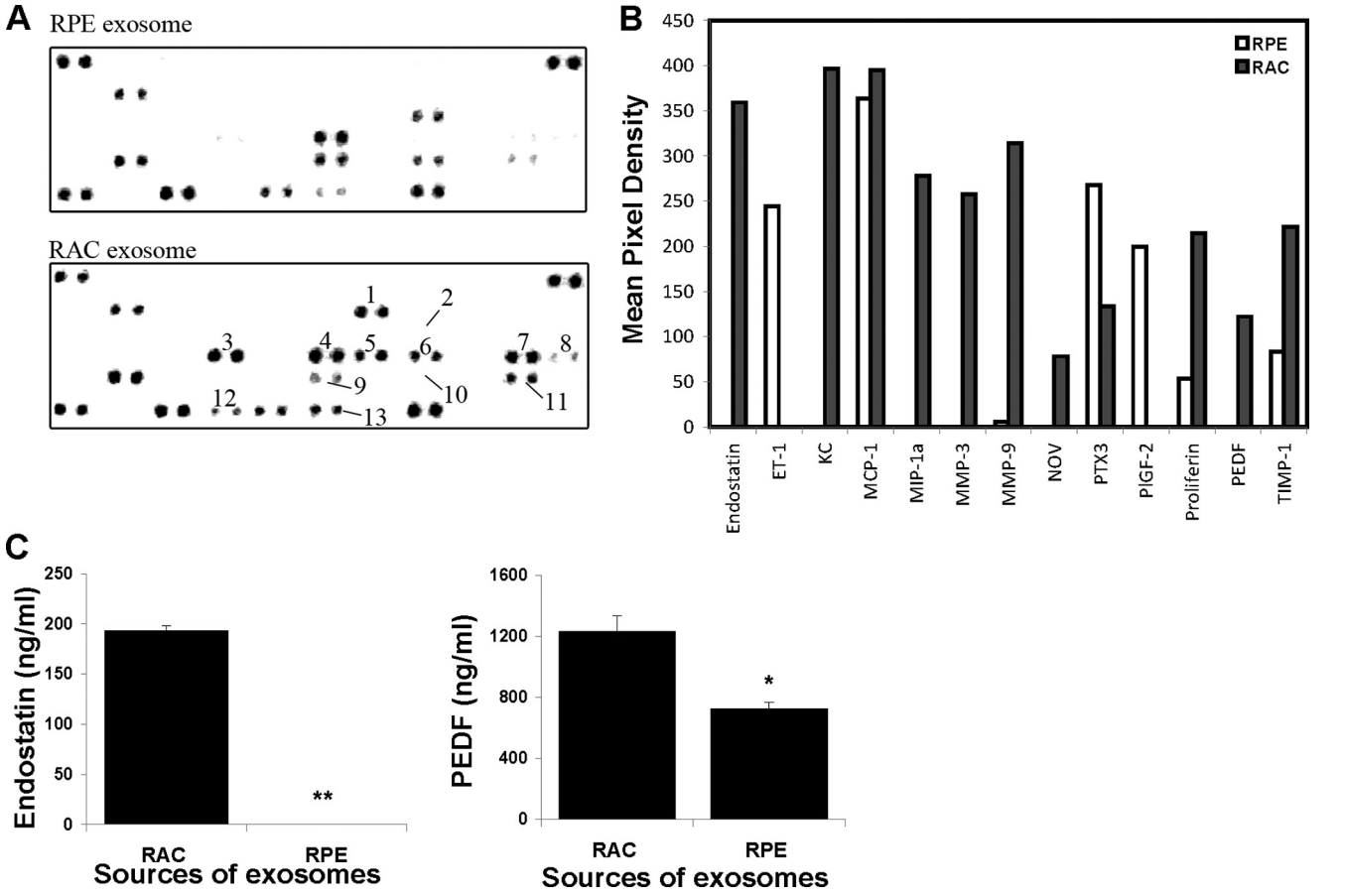

FIGURE 7. **Differences of angiogenic related protein expression between RAC exosomes and RPE exosomes.** Exosome extracts of RPE and RACs were incubated with angiogenesis antibody array according to the manufacturer's instructions. *A*, the *numbers* are indicated as differences in the expression of proteins between RAC and RPE exosomes. These are *1*, endostatin; *2*, ET-1; *3*, KC; *4*, MIP-1α; *5*, MMP-3; *6*, MMP-9; *7*, NOV; *8*, PTX3; *9*, PlGF-2; *10*, proliferin; *11*, PEDF; and *12*, TIMP-1. *B*, graphs represent quantification of antibody array using ImageJ software (National Institutes of Health). *C*, the levels of endostatin and PEDF in exosomes of RAC and RPE were quantitated by ELISA.

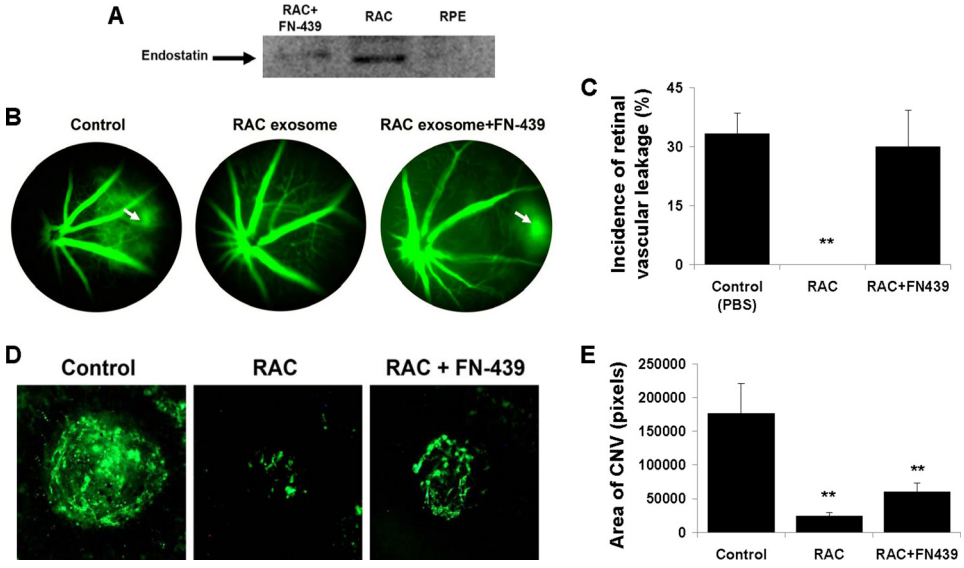

FIGURE 8. **Endostatin in RAC exosomes is responsible for suppression of retinal vessel leakage.** *A*, endostatin level in the exosomes of RACs treated with or without FN-439 and RPE was examined by Western blotting using anti-endostatin Ab. *B–E*, PBS or exosomes derived from RACs treated with or without FN-439 were periocularly injected daily into mice with laser-induced CNV. After 7 days, retinal vascular leakage was determined (*B* and *C*), representative spot of CNV was photographed (*D*), and the average area of CNV in all four laser spots of six mice was measured (*E*) in choroidal flat mounts. **, $p < 0.01$ compared with control group treated with PBS in one-way ANOVA. *Error bars* indicate S.E.

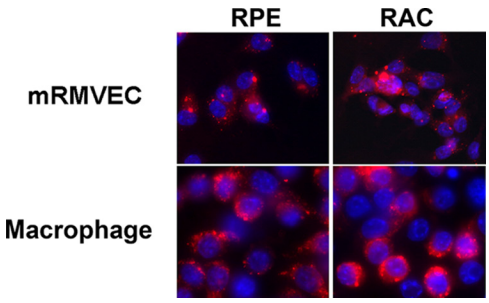

FIGURE 9. **Internalization of exosomes by macrophages and mRMVECs.** PKH-26 (*red*)-labeled exosomes were incubated with either mRMVECs or macrophages on a slide chamber for 2 h at 37 °C. Thereafter, the cells were washed with PBS, fixed in ethanol, stained with DAPI, and observed under a fluorescent microscope (magnification, ×40).

cular permeability is possibly an up-regulation of tight junction proteins (34). Nevertheless, it cannot be excluded that FN-439, an MMP inhibitor, inhibits other proteins that are responsible for suppression of vascular leakage.

It has recently been reported that exosome-encapsulated anti-inflammatory drugs can be transported from the nares to the brain to treat CNS inflammatory diseases (39). In a like manner, periocular injection of exosomes resulted in their rapid delivery from the subtenon space into the choroid and retina (Fig. 2). Hence, the periocular injection of exosomes for therapeutic purposes may provide a safe route of administration that avoids the discomfort and risk of serious adverse events such as infectious endophthalmitis caused by intravitreal injection, the most common route used for the delivery of anti-VEGF medications. Moreover, the periocular injection of exosomes avoids the dilution effect associated with systemic delivery (40–43). However, the ability of nanometer-sized RAC exosomes to penetrate via topical administration (44) or through slow release from an extraocular polymer should be explored to avoid the need for frequent intravitreal or extraocular injections.

In conclusion, we have demonstrated that exosomes released from RACs target two major cells, macrophages and vascular endothelial cells, which are involved in the angiogenic process. RAC exosomes contain known antiangiogenic proteins such as endostatin and PEDF that may play a role in the inhibition of laser-induced CNV in the mouse. Hence, RAC exosomes have the potential to provide a novel form of therapy for exudative AMD, as well as other angiogenic diseases. Fundamental studies need to be conducted to further our understanding of the constituents of exosomes derived from RACs.

Acknowledgment—We thank Tom Barkas for editorial assistance.

REFERENCES

1. Théry, C., Zitvogel, L., and Amigorena, S. (2002) Exosomes: composition, biogenesis and function. *Nat. Rev. Immunol.* **2,** 569–579
2. Zhang, H. G., and Grizzle, W. E. (2011) Exosomes and cancer: a newly described pathway of immune suppression. *Clin. Cancer Res.* **17,** 959–964
3. Yang, M., Chen, J., Su, F., Yu, B., Su, F., Lin, L., Liu, Y., Huang, J. D., and Song, E. (2011) Microvesicles secreted by macrophages shuttle invasion-potentiating microRNAs into breast cancer cells. *Mol. Cancer* **10,** 117
4. Martinez, M. C., and Andriantsitohaina, R. (2011) Microparticles in angiogenesis: therapeutic potential. *Circ. Res.* **109,** 110–119
5. Bussolati, B., Grange, C., and Camussi, G. (2011) Tumor exploits alternative strategies to achieve vascularization. *FASEB J.* **25,** 2874–2882
6. Park, J. E., Tan, H. S., Datta, A., Lai, R. C., Zhang, H., Meng, W., Lim, S. K., and Sze, S. K. (2010) Hypoxic tumor cell modulates its microenvironment to enhance angiogenic and metastatic potential by secretion of proteins and exosomes. *Mol. Cell. Proteomics* **9,** 1085–1099
7. Martínez, M. C., Larbret, F., Zobairi, F., Coulombe, J., Debili, N., Vainchenker, W., Ruat, M., and Freyssinet, J. M. (2006) Transfer of differentiation signal by membrane microvesicles harboring hedgehog morphogens. *Blood* **108,** 3012–3020
8. Couch, S. M., and Bakri, S. J. (2011) Review of combination therapies for neovascular age-related macular degeneration. *Semin. Ophthalmol.* **26,** 114–120
9. Witmer, A. N., Vrensen, G. F.., Van Noorden, C. J., and Schlingemann, R. O. (2003) Vascular endothelial growth factors and angiogenesis in eye disease. *Prog. Retin. Eye Res.* **22,** 1–29
10. Takeda, A., Baffi, J. Z., Kleinman, M. E., Cho, W. G., Nozaki, M., Yamada, K., Kaneko, H., Albuquerque, R. J., Dridi, S., Saito, K., Raisler, B. J., Budd, S. J., Geisen, P., Munitz, A., Ambati, B. K., Green, M. G., Ishibashi, T., Wright, J. D., Humbles, A. A., Gerard, C. J., Ogura, Y., Pan, Y., Smith, J. R., Grisanti, S., Hartnett, M. E., Rothenberg, M. E., and Ambati, J. (2009) CCR3 is a therapeutic and diagnostic target for neovascular age-related macular degeneration. *Nature* **460,** 225–230
11. Mullins, R. F., Aptsiauri, N., and Hageman, G. S. (2001) Structure and composition of drusen associated with glomerulonephritis: implications for the role of complement activation in drusen biogenesis. *Eye* **15,** 390–395
12. Johnson, L. V., Leitner, W. P., Rivest, A. J., Staples, M. K., Radeke, M. J., and Anderson, D. H. (2002) The Alzheimer's Aβ-peptide is deposited at sites of complement activation in pathologic deposits associated with aging and age-related macular degeneration. *Proc. Natl. Acad. Sci. U.S.A.* **99,** 11830–11835
13. Penfold, P. L., Madigan, M. C., Gillies, M. C., and Provis, J. M. (2001) Immunological and aetiological aspects of macular degeneration. *Prog. Retin. Eye Res.* **20,** 385–414
14. Lavalette, S., Raoul, W., Houssier, M., Camelo, S., Levy, O., Calippe, B., Jonet, L., Behar-Cohen, F., Chemtob, S., Guillonneau, X., Combadière, C., and Sennlaub, F. (2011) Interleukin-1β inhibition prevents choroidal neovascularization and does not exacerbate photoreceptor degeneration. *Am. J. Pathol.* **178,** 2416–2423
15. Chan, C. C., Ross, R. J., Shen, D., Ding, X., Majumdar, Z., Bojanowski, C. M., Zhou, M., Salem, N., Jr., Bonner, R., and Tuo, J. (2008) Ccl2/Cx3cr1-deficient mice: an animal model for age-related macular degeneration. *Ophthalmic Res.* **40,** 124–128
16. Fujimoto, T., Sonoda, K. H., Hijioka, K., Sato, K., Takeda, A., Hasegawa, E., Oshima, Y., and Ishibashi, T. (2010) Choroidal neovascularization enhanced by *Chlamydia pneumoniae* via Toll-like receptor 2 in the retinal pigment epithelium. *Invest. Ophthalmol. Vis. Sci.* **51,** 4694–4702
17. Cho, Y., Wang, J. J., Chew, E. Y., Ferris, F. L., 3rd, Mitchell, P., Chan, C. C., and Tuo, J. (2009) Toll-like receptor polymorphisms and age-related macular degeneration: replication in three case-control samples. *Invest. Ophthalmol. Vis. Sci.* **50,** 5614–5618
18. Weismann, D., Hartvigsen, K., Lauer, N., Bennett, K. L., Scholl, H. P., Charbel Issa, P., Cano, M., Brandstätter, H., Tsimikas, S., Skerka, C., Superti-Furga, G., Handa, J. T., Zipfel, P. F., Witztum, J. L., and Binder, C. J. (2011) Complement factor H binds malondialdehyde epitopes and protects from oxidative stress. *Nature* **478,** 76–81
19. Totan, Y., Yağci, R., Bardak, Y., Ozyurt, H., Kendir, F., Yilmaz, G., Sahin, S., and Sahin Tiğ, U. (2009) Oxidative macromolecular damage in age-related macular degeneration. *Curr. Eye Res.* **34,** 1089–1093
20. Ethen, C. M., Reilly, C., Feng, X., Olsen, T. W., and Ferrington, D. A. (2007) Age-related macular degeneration and retinal protein modification by 4-hydroxy-2-nonenal. *Invest. Ophthalmol. Vis. Sci.* **48,** 3469–3479
21. Jiang, G., Ke, Y., Sun, D., Han, G., Kaplan, H. J., and Shao, H. (2008) Reactivation of uveitogenic T cells by retinal astrocytes derived from experimental autoimmune uveitis-prone B10RIII mice. *Invest. Ophthalmol. Vis. Sci.* **49,** 282–289
22. Jiang, G., Sun, D., Kaplan, H. J., and Shao, H. (2012) Retinal astrocytes

pretreated with NOD2 and TLR2 ligands activate uveitogenic T cells. *PLoS ONE* **7,** e40510
23. Jiang, G., Ke, Y., Sun, D., Wang, Y., Kaplan, H. J., and Shao, H. (2009) Regulatory role of TLR ligands on the activation of autoreactive T cells by retinal astrocytes. *Invest. Ophthalmol. Vis. Sci.* **50,** 4769–4776
24. Liu, Y., Clem, B., Zuba-Surma, E. K., El-Naggar, S., Telang, S., Jenson, A. B., Wang, Y., Shao, H., Ratajczak, M. Z., Chesney, J., and Dean, D. C. (2009) Mouse fibroblasts lacking RB1 function form spheres and undergo reprogramming to a cancer stem cell phenotype. *Cell Stem Cell* **4,** 336–347
25. Liu, C., Yu, S., Zinn, K., Wang, J., Zhang, L., Jia, Y., Kappes, J. C., Barnes, S., Kimberly, R. P., Grizzle, W. E., and Zhang, H. G. (2006) Murine mammary carcinoma exosomes promote tumor growth by suppression of NK cell function. *J. Immunol.* **176,** 1375–1385
26. Bora, P. S., Hu, Z., Tezel, T. H., Sohn, J. H., Kang, S. G., Cruz, J. M., Bora, N. S., Garen, A., and Kaplan, H. J. (2003) Immunotherapy for choroidal neovascularization in a laser-induced mouse model simulating exudative (wet) macular degeneration. *Proc. Natl. Acad. Sci. U.S.A.* **100,** 2679–2684
27. Ray, A., and Dittel, B. N. (2010) Isolation of mouse peritoneal cavity cells. *J. Vis. Exp.* **28,** 1488
28. Liao, T., Ke, Y., Shao, W. H., Haribabu, B., Kaplan, H. J., Sun, D., and Shao, H. (2006) Blockade of the interaction of leukotriene b4 with its receptor prevents development of autoimmune uveitis. *Invest. Ophthalmol. Vis. Sci.* **47,** 1543–1549
29. Patel, M., and Chan, C. C. (2008) Immunopathological aspects of age-related macular degeneration. *Semin. Immunopathol.* **30,** 97–110
30. Cao, X., Shen, D., Patel, M. M., Tuo, J., Johnson, T. M., Olsen, T. W., and Chan, C. C. (2011) Macrophage polarization in the maculae of age-related macular degeneration: a pilot study. *Pathol. Int.* **61,** 528–535
31. Wang, Y., Wang, V. M., and Chan, C. C. (2011) The role of anti-inflammatory agents in age-related macular degeneration (AMD) treatment. *Eye* **25,** 127–139
32. Shichita, T., Hasegawa, E., Kimura, A., Morita, R., Sakaguchi, R., Takada, I., Sekiya, T., Ooboshi, H., Kitazono, T., Yanagawa, T., Ishii, T., Takahashi, H., Mori, S., Nishibori, M., Kuroda, K., Akira, S., Miyake, K., and Yoshimura, A. (2012) Peroxiredoxin family proteins are key initiators of post-ischemic inflammation in the brain. *Nat. Med.* **18,** 911–917
33. Luhmann, U. F., Robbie, S., Munro, P. M., Barker, S. E., Duran, Y., Luong, V., Fitzke, F. W., Bainbridge, J. W., Ali, R. R., and MacLaren, R. E. (2009) The drusenlike phenotype in aging Ccl2-knockout mice is caused by an accelerated accumulation of swollen autofluorescent subretinal macrophages. *Invest. Ophthalmol. Vis. Sci.* **50,** 5934–5943
34. Marneros, A. G., She, H., Zambarakji, H., Hashizume, H., Connolly, E. J., Kim, I., Gragoudas, E. S., Miller, J. W., and Olsen, B. R. (2007) Endogenous endostatin inhibits choroidal neovascularization. *FASEB J.* **21,** 3809–3818
35. Huber, M., and Wachtlin, J. (2012) Vitreous levels of proteins implicated in angiogenesis are modulated in patients with retinal or choroidal neovascularization. *Ophthalmologica* **228,** 188–193
36. Mirochnik, Y., Aurora, A., Schulze-Hoepfner, F. T., Deabes, A., Shifrin, V., Beckmann, R., Polsky, C., and Volpert, O. V. (2009) Short pigment epithelial-derived factor-derived peptide inhibits angiogenesis and tumor growth. *Clin. Cancer Res.* **15,** 1655–1663
37. Johnson, M. D., Kim, H. R., Chesler, L., Tsao-Wu, G., Bouck, N., and Polverini, P. J. (1994) Inhibition of angiogenesis by tissue inhibitor of metalloproteinase. *J. Cell. Physiol.* **160,** 194–202
38. Egeblad, M., and Werb, Z. (2002) New functions for the matrix metalloproteinases in cancer progression. *Nat. Rev. Cancer* **2,** 161–174
39. Zhuang, X., Xiang, X., Grizzle, W., Sun, D., Zhang, S., Axtell, R. C., Ju, S., Mu, J., Zhang, L., Steinman, L., Miller, D., and Zhang, H. G. (2011) Treatment of brain inflammatory diseases by delivering exosome encapsulated anti-inflammatory drugs from the nasal region to the brain. *Mol. Ther.* **19,** 1769–1779
40. Delcayre, A., and Le Pecq, J. B. (2006) Exosomes as novel therapeutic nanodevices. *Curr. Opin. Mol. Ther.* **8,** 31–38
41. Hao, S., Moyana, T., and Xiang, J. (2007) Review: cancer immunotherapy by exosome-based vaccines. *Cancer Biother. Radiopharm.* **22,** 692–703
42. Lebreton, A., and Séraphin, B. (2008) Exosome-mediated quality control: substrate recruitment and molecular activity. *Biochim. Biophys. Acta* **1779,** 558–565
43. Lorentzen, E., and Conti, E. (2006) The exosome and the proteasome: nano-compartments for degradation. *Cell* **125,** 651–654
44. Courrier, H. M., Butz, N., and Vandamme, T. F. (2002) Pulmonary drug delivery systems: recent developments and prospects. *Crit. Rev. Ther. Drug Carrier Syst.* **19,** 425–498